Spatial Variability and Interpolation of Stochastic Weather Simulation Model Parameters

GREGORY L. JOHNSON

U.S. Department of Agriculture Natural Resources Conservation Service, National Water and Climate Center, Portland, Oregon

CHRISTOPHER DALY AND GEORGE H. TAYLOR

Oregon State University, Corvallis, Oregon

CLAYTON L. HANSON

U.S. Department of Agriculture Agricultural Research Service, Northwest Watershed Research Center, Boise, Idaho

(Manuscript received 16 March 1999, in final form 19 July 1999)

ABSTRACT

The spatial variability of 58 precipitation and temperature parameters from the ''generation of weather elements for multiple applications'' (GEM) weather generator has been investigated over a region of significant complexity in topography and climate. GEM parameters were derived for 80 climate stations in southern Idaho and southeastern Oregon. A technique was developed and used to determine the GEM parameters from high-elevation snowpack telemetry stations that report precipitation in nonstandard 2.5-mm (versus 0.25 mm) increments. Important dependencies were noted between most of these parameters and elevation (both domainwide and local), location, and other factors. The ''parameter-elevation regressions on independent slopes model'' (PRISM) spatial modeling system was used to develop approximate 4-km gridded data fields of each of these parameters. A feature was developed in PRISM that models temperatures above and below mean inversions differently. Examples of the spatial fields derived from this study and a discussion of the applications of these spatial parameter fields are included.

1. Introduction

Stochastic weather simulation models, or ''weather generators,'' increasingly are used for a broad spectrum of applications. Originally developed to deliver serially complete climate datasets for biological and hydrological models, weather generators have gained wider acceptance and have been utilized for a variety of purposes in recent years, including their use in climate change investigations (Katz 1996; Mearns et al. 1996). Because of their ability to mimic the true climate of a location, their ease of use, and their functionality for generating long time series of weather data quickly and without many of the problems associated with real climate data (missing values, errors), the popularity of weather generators continues to grow.

Corresponding author address: Greg Johnson, Applied Climatologist, USDA-NRCS, 101 Main St. Suite 1600, Portland, OR 97204-3224.
E-mail: gjohnson@wcc.nrcs.usda.gov

These multivariate stochastic models of weather and climate traditionally have been point models. Model parameters are derived from available climatological data at a location, and the generated time series from the model typically is applied to some small region around this station in which the climate is assumed to be essentially the same.

In practice, climate rarely is homogeneous spatially, rendering the generated time series inappropriate for application to places even a few kilometers distant (in an extreme case). The usefulness and applicability of the stochastic model thus are reduced greatly. In fact, one of the reasons chiefly touted for using generated time series is that they can be produced for locations with no available climate data (Richardson and Wright 1984; Woolhiser et al. 1988; Nicks and Gander 1994; Hanson et al. 1994). As climate increases in spatial complexity, however, it becomes less likely that parameters for a specific location will be applicable to any surrounding location.

The spatial distribution of stochastic simulation model parameters only recently has been investigated. Mean

and seasonally varying components of the five primary parameters of a daily precipitation model were hypothesized to have regional characteristics that lead to the capability of isopleth mapping (Woolhiser and Pegram 1979). Richardson (1981) also thought this capability was possible, and, in the user's guide to his weather generator (WGEN) model (Richardson and Wright 1984), maps of important parameters across the United States were developed based on climate descriptions from 31 temperature and solar radiation stations and 139 precipitation stations. Some parameters were found to be constant and/or not highly related to geographic location, and others had significant spatial variability. In the WGEN user's guide it is stated that ''parameters for other locations may be obtained by interpolation of values given in the same table.'' This approach assumes, of course, straightforward and consistent parameter gradients between stations, an assumption which often is invalid, especially in mountainous regions.

There thus is motivation for the development of some kind of parameter interpolation method that is sensitive to the major forcing mechanisms that produce spatial variability; namely, topography (elevation, aspect, slope), scale, and proximity to larger water bodies. With such an interpolation procedure established, gridded fields of weather generator parameters can be produced, and it then becomes possible to generate time series at any number of locations, regardless of the availability of climate data. These time series will be uncorrelated temporally; however, accurate point time series are still extremely useful, and needed, for a great number of applications.

The concept proposed and tested here seeks to examine the spatial variability of various stochastic weather generator parameters and then to use a spatial modeling system to produce gridded fields of these parameters. The methodology also should result in linkages between parameter fields (layers) so that a user can select a location of interest, extract all necessary weather-generator parameters for that location and ingest them into the model, and then generate a desired-length time series of weather for the location (individual grid cell), all with a simple point-and-click configuration.

2. Models used and their characteristics

To develop and to test these ideas, a stochastic weather generator model and an ''intelligent'' interpolation model were needed. The weather generator model chosen was the ''generation of weather elements for multiple applications'' (GEM), developed by researchers with the U.S. Department of Agriculture Agricultural Research Service (USDA–ARS), and previously known as WGEN (Richardson and Wright 1984) and USCLIMATE (Hanson et al. 1994). The interpolation model used was the ''parameter-elevation regressions on independent slopes model'' (PRISM), developed by researchers at Oregon State University (Daly et al. 1994).

a. GEM

GEM was chosen because of its proven ability to replicate successfully most aspects of the real climate, including the preservation of serial and cross-element correlations. GEM produces a daily time series of precipitation, maximum and minimum air temperature, solar radiation, mean daily dewpoint, and wind speed. GEM uses a Markov chain–mixed-exponential model for precipitation generation and a multivariate model for generating temperature and other elements such as solar radiation and dewpoint (Hanson and Johnson 1998). The generated elements of the multivariate model are dependent on precipitation occurrence, prescribed by the Markov model. Precipitation amounts are drawn from a mixed-exponential distribution (Smith and Schreiber 1974). This particular distribution has been found to be superior in matching overall aspects of precipitation (Wilks 1998; Foufoula-Georgiou and Lettenmaier 1987) in comparison with other statistical distributions, including the exponential model, used in Richardson's first version of this model (Richardson 1981), and the two-parameter gamma, used several years later by Richardson and Wright (1984) in the WGEN version of the model.

A strength of GEM is the multivariate structure of the model, preserving the serial and cross-element correlations between all nonprecipitation elements. Richardson (1981) developed this portion of the model, based on work by Matalas (1967), who first applied it to stream flow generation at multiple sites. A complete summary of this methodology is given in Johnson et al. (1996). In short, temperature and other nonprecipitation elements are generated based on daily mean and standard deviation values, the previous day's value, and the correlation with other elements. Serial and cross-element correlations are assumed to be constant temporally and spatially; for example, one set of values is used for all locations in all times of the year. In a study of the dependence structure of daily temperature and solar radiation, Richardson (1982) found that the serial and cross-correlation coefficients in the multivariate model showed relatively small spatial variability. Preliminary analysis has shown that site-specific serial and cross-correlation coefficients can be important in generating some elements at some locations at certain times of the year, and that there can be some spatial variability, especially in mountainous regions (Hayhoe 1998; Parlange and Katz 2000). For purposes of simplicity, however, the original, national-average correlation-coefficient values of temperature calculated by Richardson and used in WGEN were adopted in this study to reduce the number of parameters to be derived and interpolated without greatly compromising model performance. Certainly, for best model replication of true climate, separate correlation coefficients for individual locations and for different seasons or months would be recommended.

Investigation of these parameters should be pursued in future research.

Johnson et al. (1996) found that GEM reproduced climatic means and precipitation variance adequately. Variance replication of both temperature and solar radiation was locationally dependent but generally between 70% and 90% of historical values. Extreme values of precipitation, temperature, and solar radiation were reproduced less accurately but were also highly a function of location and season.

b. PRISM

PRISM is a climate analysis system that uses point data, a digital elevation model (DEM), and other spatial datasets to generate gridded estimates of annual, monthly, and event-based climatic parameters (Daly et al. 1994, 1997). Originally developed in 1991 for precipitation estimation, PRISM has been generalized and applied successfully to temperature, growing degree days, and frost dates (Taylor et al. 1997). It has been used extensively to map precipitation and minimum and maximum temperature over the United States, Canada, and other countries (Kittel et al. 1997; Parzybok et al. 1997). PRISM was developed to estimate climate successfully in areas such as mountainous regions where topography and other factors produce significant variability in climate. The effects of terrain on climate play a central role in the model's conceptual framework.

PRISM is not a static system of equations; rather, it is a coordinated set of rules, decisions, and calculations designed to accommodate the decision-making process that an expert climatologist would invoke when creating a climate map. The PRISM system is kept as open-ended and flexible as possible to ensure that information gathered from applying PRISM to a new region or climate element is integrated into the knowledge base.

PRISM makes the assumption that, on a local hill slope, elevation is the primary predictor of many climate elements. For each grid cell, PRISM calculates weighted linear relationships with elevation, using station data as the independent data source. Each station's value is weighted in the regression based on several factors, including distance from the grid cell, difference in elevation between the station and the grid cell, vertical layer of the station versus vertical layer of the grid cell [see discussion of minimum temperature prediction, section 4b(2)], and several others. For a complete overview of the current PRISM modeling system consult C. Daly (1999, manuscript submitted to *Climate Res.*), or the PRISM Guide Book document, which, at the time of writing, was available at http://www.ocs.orst.edu/prism/prism_new.html.

3. GEM parameters and their derivation

Precipitation and maximum and minimum air temperature (Tmax, Tmin) were the elements chosen for testing in this study, because these three elements were recorded at all of the observation sites used in this study (see section 4). A complete discussion of the precipitation and temperature parameters used by the GEM model is given in Johnson et al. (1996) and Hanson et al. (1994), with GEM referenced by the previous program name of USCLIMATE.

TABLE 1. Parameters derived and interpolated in this study, and their meanings.

Precipitation	
p_{00}	Conditional probability (from 0 to 1) for a dry day (denoted by 0) following a dry day. Equal to $1 - p_{01.}$ Twelve separate monthly values.
p_{10}	Conditional probability (from 0 to 1) for a dry day (denoted by 0) following a wet day. Equal to $1 - p_{11.}$ Twelve separate monthly values.
β	Mean value of the smaller (lower) exponential distribution (mm) of the mixed-exponential distribution. Twelve separate monthly values.
α	Weighting factor (from 0 to 1) used to determine the proportion of the total distribution of daily precipitation amounts falling into either the lower (β) or the upper (δ) portions of the mixed-exponential distribution.
μ	Mean daily precipitation (mm). Twelve separate monthly values.
Temperature	
Mean Tmax_d	Mean annual maximum temperature on dry days (°C).
Amp Tmax	Amplitude of the first (annual) harmonic of mean maximum temperature (°C) for wet and dry days.
Mean CV Tmax	Mean annual coefficient of variation of maximum temperature (°C) for wet and dry days.
Amp CV Tmax	Amplitude of the first (annual) harmonic of the mean coefficient of variation of maximum temperature (°C) for wet and dry days.
Mean Tmax_w	Mean annual maximum temperature on wet days (°C).
Mean Tmin	Mean annual minimum temperature on wet and dry days (°C).
Amp Tmin	Amplitude of the first (annual) harmonic of mean minimum temperature (°C) for wet and dry days.
Mean CV Tmin	Mean annual coefficient of variation of minimum temperature (°C) for wet and dry days.
Amp CV Tmin	Amplitude of the first (annual) harmonic of the mean coefficient of variation of minimum temperature (°C) for wet and dry days.

Forty-nine precipitation and 9 temperature parameters were necessary for proper generation of GEM time series; thus, a total of 58 PRISM-produced parameter layers were developed using these procedures (Table 1). Precipitation occurrence parameters used in GEM were p_{00} and p_{10}, representing the conditional probabilities of a dry day (subscript 0) following a dry day and a dry day following a wet day (subscript 1), respectively. Parameters used for generating the amount of precipitation on any given day, taken from the mixed-exponential distribution, were μ, the mean amount of precipitation on a wet day; β, the mean value of the smaller expo-

nential distribution; δ, the mean value of the larger exponential distribution; and α, a weighting parameter used to define the relative contribution of each of the smaller and larger exponential distributions, with values between 0 and 1. These parameters were related to one another by the relation

$$\mu(n) = \alpha(n)\beta(n) + [1 - \alpha(n)]\delta(n), \quad (1)$$

on any day n. Larger values of β and/or δ will thus result in larger values of μ, meaning more precipitation on a wet day.

Previous versions of the model used an optimization routine to select only significant annual harmonics and Fourier coefficients, but spatial variability of these parameters was found to be complex. Instead, discrete, monthly parameter values were derived, analyzed, and interpolated using PRISM for all parameters except α, which showed no significant seasonal changes.

Parameters used for generating temperature values were the annual mean and amplitude values of Tmax and Tmin, and their associated coefficients of variation. Earlier studies have shown that it is important to parameterize the annual mean Tmax differently for wet and dry days (Tmax_w, Tmax_d) and this convention was followed here.

Two separate programs are used for GEM parameter estimation. These programs are commonly referred to as AGUA, for precipitation parameter determination, and GENPAR, for deriving temperature (and all other) parameters. AGUA is an integration of several computer codes by several authors, including Woolhiser and Roldan (1982a,b, 1986), and Hanson et al. (1994). Parameter values are estimated by numerical optimization of the log likelihood function (maximum likelihood estimation), as described by Woolhiser and Pegram (1979), for each of 26 14-day periods of the year. AGUA was modified for this study so that the requirement for serially complete datasets was relaxed, allowing a greater number of stations to be used, and the time associated with data cleanup and estimation of missing values was reduced.

The seasonal variation of GEM precipitation parameters originally was described using a polar form of a finite Fourier series (Woolhiser and Pegram 1979). The original AGUA program delivered annual mean and significant harmonic values for p_{00}, p_{10}, μ, and β. Significant harmonics were determined using a maximum likelihood procedure. In most cases, the seasonal variation of a parameter at a location could be described by two or three harmonics. The program examined the first six harmonics for significance, however, and often the significant harmonics determined by likelihood ratio tests were different for nearby locations. Spatial interpretation of these amplitudes and phase angles thus was difficult, at best, especially because of zero values at locations where a particular harmonic was not deemed to be significant by the procedure. Therefore, although the original procedure optimized harmonic values at a particular location, a more spatially robust method of describing the seasonally fluctuating nature of these parameters was needed in regions in which terrain and climate are complex.

A first option, discussed by Woolhiser and Pegram (1979) and addressed by Woolhiser and Roldan (1986), involves calculating the first few nonoptimized harmonics of each parameter and then mapping these amplitudes and phase angles. For all locations in this study, the annual mean and first three harmonics of each parameter were derived and their spatial characteristics were examined. Although this method eliminated all zero values, a second problem arose because of the spatial interpretation of the phase angles. For instance, nearly all high-elevation stations in this study had first-harmonic phase angles that maximized p_{10} and minimized μ in the summer. At lower elevations, though, the seasonal pattern was much less clear. Often, the range of phase angles corresponding to the first harmonic at high elevations was associated with the second or third harmonic (or, in a few cases, was not even significant) at low elevations. Again, spatial interpretation and interpolation were difficult.

A second option was developed and adopted for this study. Time-discrete (monthly) parameter values were derived for each site, which made for significantly easier spatial interpolation. After interpolation, daily values were determined by fitting a Fourier series (mean and three harmonics) to the monthly values. Tests found that no appreciable reduction in model performance occurred when this procedure was adopted, and spatial interpretation and interpolation were possible. An example of a monthly parameter and its relationship to monthly precipitation is shown in Fig. 1, depicting p_{10} against mean December precipitation, along with a best-fit line through the 80 station values (also, see appendix).

AGUA-derived precipitation parameters using snowpack telemetry (SNOTEL) data were not congruent with parameters derived from National Oceanic and Atmospheric Administration (NOAA) data because of differences in the periods of record from the two networks and differences in the minimum threshold amount in the two observing systems (2.5 versus 0.25 mm). A description of a method developed to calculate consistent parameters from SNOTEL data is given in the appendix.

The GENPAR program was developed by Richardson (1981) for temperature and solar radiation parameter estimation, and one version of the program was printed as an appendix in Richardson and Wright (1984). Mean, standard deviation, and coefficient of determination values for each of 13 28-day periods were derived from a serially complete dataset (the same one used for AGUA), and then these 13 values were fit with a single-harmonic Fourier series. For this study, GENPAR also was modified to allow less-than–serially complete datasets to be used. In all cases, however, the datasets used

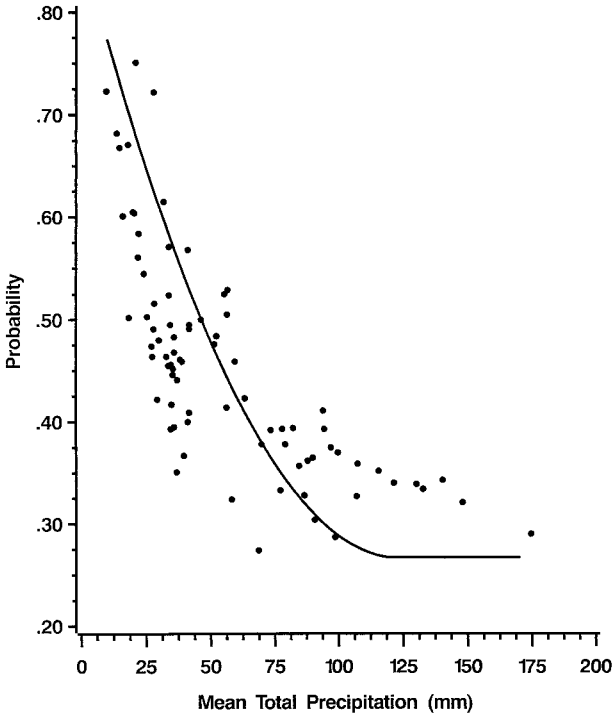

FIG. 1. Plot of p_{10} vs Dec mean precipitation at all 80 stations, with second-order polynomial curve shown, used for SNOTEL parameter estimation. Curve is forced to level off at minimum threshold value. The variance $r^2 = 0.93$.

for both GENPAR and AGUA were subjected to quality control to remove or correct erroneous values.

4. Regional test and discussion

a. Regional description and sources of data

This methodology was tested over an approximate 60 000 km^2 area of southern and central Idaho and southeastern Oregon (Fig. 2). This region is diverse in topography and climate. The broad Snake River Plain arcing east–west across most of the domain is relatively flat and low in elevation (600–1100 m) and very dry (less than 250 mm of annual precipitation). South and north of this region are mountainous sections with elevations as high as 3800 m. The variety of topography creates widely different climates, often separated by relatively small distances. The dependence of precipitation and temperature on elevation, aspect, and geographic location thus is less than straightforward and presents a significant challenge for the testing of this approach.

Eighty climate stations with sufficiently long records were utilized in this study (Table 2). Approximately 60 were NOAA Cooperative stations with generally complete 1961–93 data. An additional 17 SNOTEL stations and three ARS stations at the Reynolds Creek Experimental Watershed (RCEW) were used to provide data from high-elevation regions. Although the SNOTEL record lengths were much shorter (generally from 1983 to 1993), procedures were developed to make the SNOTEL parameters compatible and consistent with the NOAA and ARS station parameters (see section 3b).

To provide guidance for PRISM interpolation of parameters, a thorough analysis of the spatial variability of GEM parameters and their temporal characteristics was conducted first. Graphs of domainwide (all 80 stations) monthly and annual parameters versus elevation were prepared. Parameters were plotted on maps to analyze spatial patterns. Then, PRISM was used to distribute these parameter values to grid points. Fifty-eight parameter maps were derived from the PRISM interpolation of the 80 station values. Each map consisted of 7957 pixel values. Statistics that summarize PRISM performance over the entire domain then were calculated and compared with the domain-wide, average statistics derived from the raw station values.

b. Spatial variability of GEM parameters over the region, and PRISM distribution

1) PRECIPITATION

Regionwide parameter/elevation graphs revealed that elevational gradients were large for many parameters, small for others, and typically had seasonal dependencies. Mean regression slopes from PRISM were consistent with these regionwide elevational gradients. Some parameters also displayed geographic (latitude and longitude) dependencies, and others showed none. The study domain is dominated by strong, westerly flow with frequent intrusions of Pacific moisture during the winter. Summers typically are warm and very dry, with only occasional storms. More than 80% of total annual precipitation falls during the 6-month winter period at highest elevations, where most of it comes in the form of snow. At lower elevations, precipitation is distributed more evenly throughout the year.

It was hypothesized that GEM parameters that describe the occurrence and amount processes of precipitation would show a greater elevational dependence in winter. This hypothesis was true for precipitation amounts (μ) but not for occurrence parameters (p_{00} and p_{10}). For example, December p_{10} was related very poorly to elevation domainwide (Fig. 3a), but in June the relationship was much stronger (variance $r^2 = 0.49$; Fig. 3b). The significant drop in p_{10} (lack of values above 0.50) in December (Fig. 3a) likely is due to the lack of NOAA stations and dominance of SNOTEL stations at these highest elevations (see Table 2). The dry, high-elevation NOAA stations (between 1500 and 1900 m) are almost exclusively in the very dry valleys of the eastern portion of the study region, and the SNOTEL sites at these elevations across the entire domain and above 1900 m are placed strategically in protected locations that generally are representative of high-elevation, snow-accumulation locations relative to the surrounding region. This fact does not mean they are not

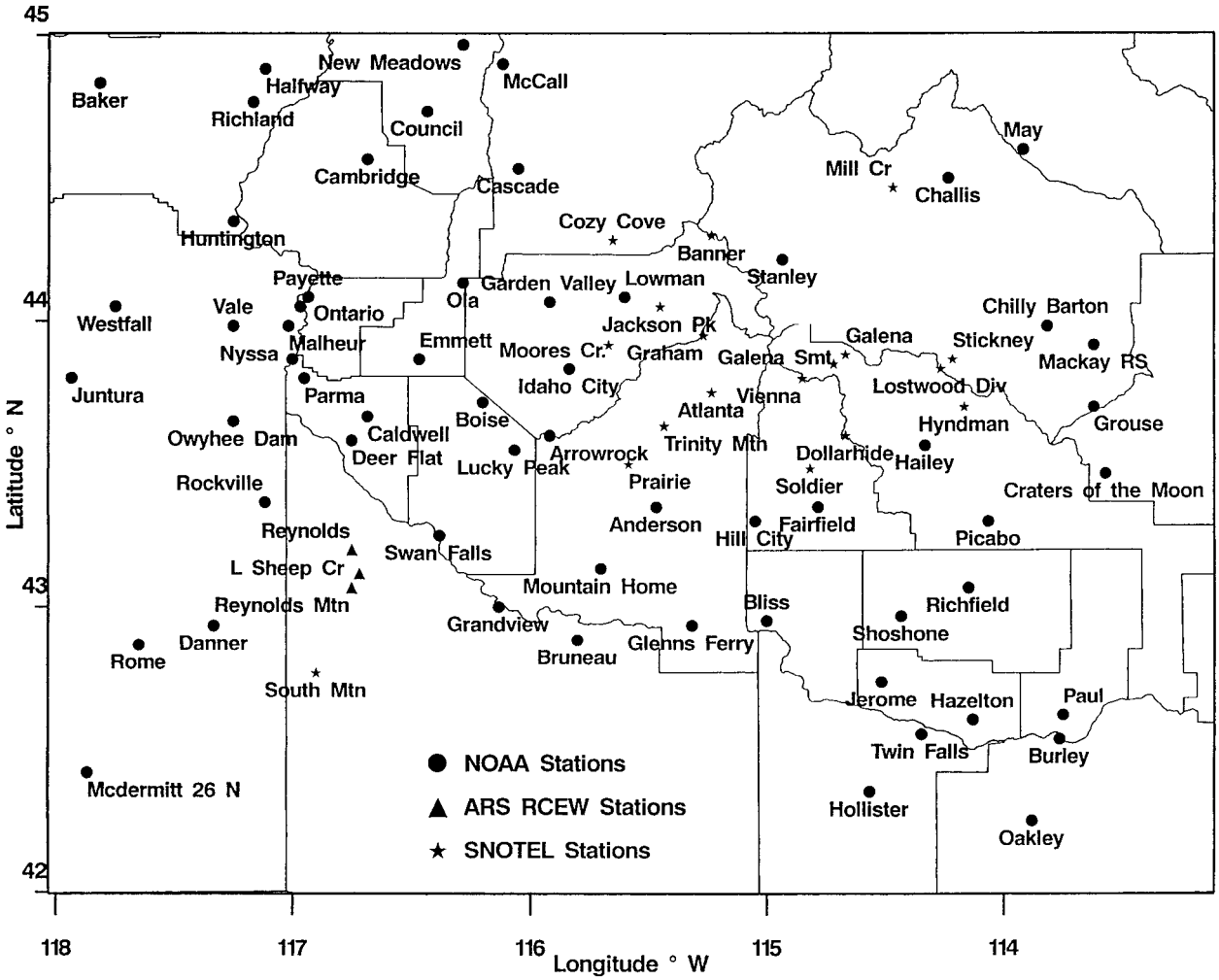

FIG. 2. Stations used in the study. Approximate scale 1:2 000 000.

representative of their location or even immediate environs; it simply means that, at equivalent elevations, the NOAA and SNOTEL sites represent very different climates, which is represented splendidly by this conditional probability graph of a dry day following a wet day in one of the wettest months.

Opposite to the behavior of p_{10}, μ was correlated more strongly with elevation in December ($r^2 = 0.34$; Fig. 3c) than in June ($r^2 = 0.19$; Fig. 3d). Thus, over this study domain, a much greater amount of precipitation per wet day falls at higher elevations in the winter. This fact is the dominating factor in enhancing mean total precipitation at higher-elevation locations, and not the occurrence process. There may be, however, significant local dependencies that are not accounted for in this domainwide analysis. Thus, a more detailed study of these local effects and parameter spatial variability was warranted. These analyses also confirmed the need for a more sophisticated interpolation procedure, such as PRISM, rather than relying on a single elevational relationship, even for a domain as relatively small as this one.

For illustration purposes, the spatial variability of four GEM precipitation parameters (p_{00}, p_{10}, μ, and β) during the month of December was examined (Fig. 4). December is one of the wetter months domainwide, and an analysis of all months revealed that parameter patterns in December were typical for most months of the year. There was significantly less spatial variability in p_{00} than in most of the other parameters, with a range between highest and lowest values across the domain of just 0.17. Highest values were found in the driest locations, as expected. Only a moderate dependency on elevation was noted (in comparison with other parameters and months), even in local areas like the ARS Reynolds Creek Watershed where the three stations are close to one another (within 15 km), yet a significant change in elevation (1200–2100 m) and mean annual precipitation (300–900 mm) is observed.

December p_{10}, μ, and β had much more spatial var-

TABLE 2. Names, locations, and other information for stations used in the study. Data periods were 1961–93 except for SNOTEL stations, which were generally 1983-93.

Station name	Lat	Long	Elevation (m)	State	Network
Anderson Dam	43°21′N	115°28′W	1183	ID	NOAA Coop
Arrowrock Dam	43°36′N	115°55′W	998	ID	NOAA Coop
Atlanta Summit	43°45′N	115°14′W	2310	ID	SNOTEL
Baker FAA AP	44°50′N	117°49′W	1027	OR	NOAA Coop
Banner Summit	44°18′N	115°14′W	2146	ID	SNOTEL
Bliss 4 NW	42°57′N	115°00′W	998	ID	NOAA Coop
Boise WSFO AP	43°43′N	116°12′W	1186	ID	NOAA Coop
Bruneau	42°53′N	115°48′W	771	ID	NOAA Coop
Burley FAA AP	42°32′N	113°46′W	1267	ID	NOAA Coop
Caldwell	43°40′N	116°41′W	722	ID	NOAA Coop
Cambridge	44°34′N	116°41′W	808	ID	NOAA Coop
Cascade 1 NW	44°32′N	116°03′W	1492	ID	NOAA Coop
Challis	44°30′N	114°14′W	1577	ID	NOAA Coop
Chilly Barton Flat	43°59′N	113°49′W	1908	ID	NOAA Coop
Council	44°44′N	116°26′W	899	ID	NOAA Coop
Cozy Cove	44°17′N	115°39′W	1640	ID	SNOTEL
Craters Of The Moon	43°28′N	113°34′W	1797	ID	NOAA Coop
Danner	42°56′N	117°20′W	1288	OR	NOAA Coop
Deer Flat Dam	43°35′N	116°45′W	765	ID	NOAA Coop
Dollarhide Summit	43°36′N	114°40′W	2566	ID	SNOTEL
Emmett 2 E	43°52′N	116°28′W	728	ID	NOAA Coop
Fairfield Ranger Station	43°21′N	114°47′W	1544	ID	NOAA Coop
Galena	43°53′N	114°40′W	2277	ID	SNOTEL
Galena Summit	43°51′N	114°43′W	2676	ID	SNOTEL
Garden Valley Research Station	44°04′N	115°55′W	978	ID	NOAA Coop
Glenns Ferry	42°56′N	115°19′W	765	ID	NOAA Coop
Graham Guard Station	43°57′N	115°16′W	1734	ID	SNOTEL
Grand View	43°00′N	116°08′W	732	ID	NOAA Coop
Grouse	43°42′N	113°37′W	1859	ID	NOAA Coop
Hailey 3 NNW	43°34′N	114°20′W	1653	ID	NOAA Coop
Halfway	44°53′N	117°07′W	814	OR	NOAA Coop
Hazelton	42°36′N	114°08′W	1237	ID	NOAA Coop
Hill City 1 W	43°18′N	115°03′W	1524	ID	NOAA Coop
Hollister	42°21′N	114°34′W	1381	ID	NOAA Coop
Huntington	44°21′N	117°15′W	643	OR	NOAA Coop
Hyndman	43°42′N	114°10′W	2268	ID	SNOTEL
Idaho City	43°50′N	115°50′W	1209	ID	NOAA Coop
Jackson Peak	44°03′N	115°27′W	2155	ID	SNOTEL
Jerome	42°44′N	114°31′W	1140	ID	NOAA Coop
Juntura 9 ENE	43°48′N	117°56′W	863	OR	NOAA Coop
Lost Wood Divide	43°50′N	114°16′W	2408	ID	SNOTEL
Lower Sheep Creek	43°07′N	116°43′W	1649	ID	ARS
Lowman	44°05′N	115°36′W	1202	ID	NOAA Coop
Lucky Peak Dam	43°33′N	116°04′W	866	ID	NOAA Coop
Mackay Ranger Station	43°55′N	113°37′W	1797	ID	NOAA Coop
Malheur Branch Experiment Station	43°59′N	117°01′W	689	OR	NOAA Coop
May	44°36′N	113°55′W	1558	ID	NOAA Coop
McCall	44°54′N	116°07′W	1532	ID	NOAA Coop
McDermitt 26 N	42°25′N	117°52′W	1359	OR	NOAA Coop
Mill Creek Summit	44°28′N	114°28′W	2682	ID	SNOTEL
Mores Creek Summit	43°55′N	115°40′W	1859	ID	SNOTEL
Mountain Home	43°08′N	115°42′W	972	ID	NOAA Coop
New Meadows	44°58′N	116°17′W	1180	ID	NOAA Coop
Nyssa	43°52′N	117°00′W	664	OR	NOAA Coop
Oakley	42°15′N	113°53′W	1402	ID	NOAA Coop
Ola 4 S	44°08′N	116°17′W	911	ID	NOAA Coop
Ontario KSRV	44°03′N	116°58′W	654	OR	NOAA Coop
Owyhee Dam	43°39′N	117°15′W	732	OR	NOAA Coop
Parma Experiment Station	43°48′N	116°57′W	677	ID	NOAA Coop
Paul 1 ENE	42°37′N	113°45′W	1283	ID	NOAA Coop
Payette	44°05′N	116°56′W	655	ID	NOAA Coop
Picabo	43°18′N	114°04′W	1486	ID	NOAA Coop
Prairie	43°30′N	115°35′W	1463	ID	SNOTEL
Reynolds	43°12′N	116°45′W	1193	ID	ARS
Reynolds Mountain	43°04′N	116°45′W	2097	ID	ARS
Richfield	43°04′N	114°09′W	1314	ID	NOAA Coop

TABLE 2. (*Continued*)

Station name	Lat	Long	Elevation (m)	State	Network
Richland	44°46′N	117°10′W	675	OR	NOAA Coop
Rockville 4 NW	43°22′N	117°07′W	1119	OR	NOAA Coop
Rome 2 NW	42°52′N	117°39′W	1039	OR	NOAA Coop
Shoshone 1 WNW	42°58′N	114°26′W	1204	ID	NOAA Coop
Soldier RS	43°29′N	114°49′W	1750	ID	SNOTEL
South Mountain	42°46′N	116°54′W	1981	ID	SNOTEL
Stanley	44°13′N	114°56′W	1911	ID	NOAA Coop
Stickney Mill	43°52′N	114°13′W	2265	ID	SNOTEL
Swan Falls Power House	43°15′N	116°23′W	709	ID	NOAA Coop
Trinity Mountain	43°38′N	115°26′W	2368	ID	SNOTEL
Twin Falls WSO	42°33′N	114°21′W	1207	ID	NOAA Coop
Vale	43°59′N	117°15′W	683	OR	NOAA Coop
Vienna Mine	43°48′N	114°51′W	2731	ID	SNOTEL
Westfall 4 NNW	44°03′N	117°45′W	957	OR	NOAA Coop

iability, and the local elevation relationship was stronger than for p_{00}. The range of observed p_{10} values over the domain was nearly 0.50. At RCEW, p_{10} decreased by 0.14 from lowest to highest elevations, and, in the eastern section of the study area, p_{10} decreased more than 0.30 over distances of less than 40 km and elevation changes of between 1200 and 1800 m. Significant, local elevation dependencies were noted domainwide, with

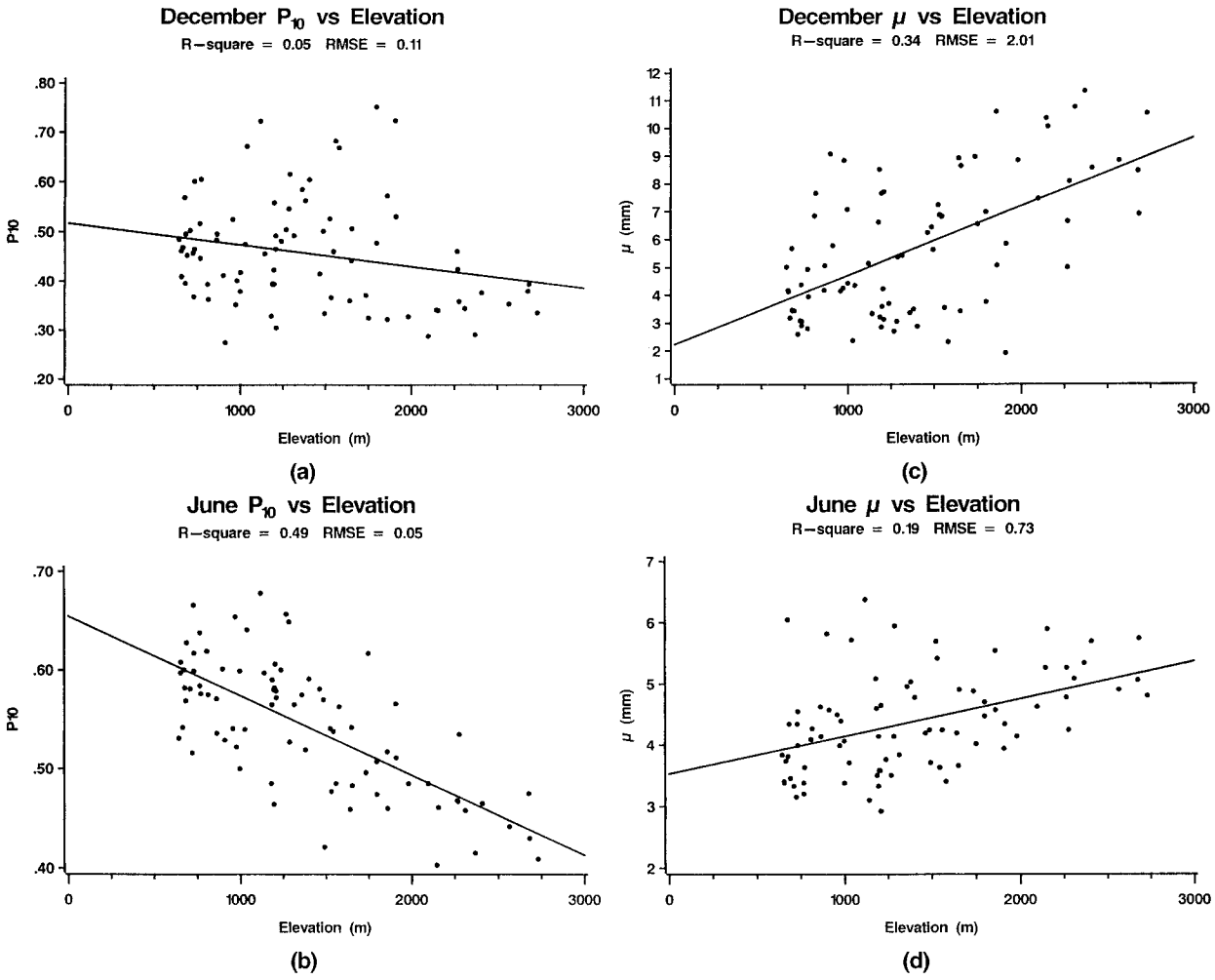

FIG. 3. Plots of p_{10} vs elevation for all 80 stations, with linear regression fit to data, for (a) Dec and (b) Jun; also shown are plots for μ for (c) Dec and (d) Jun.

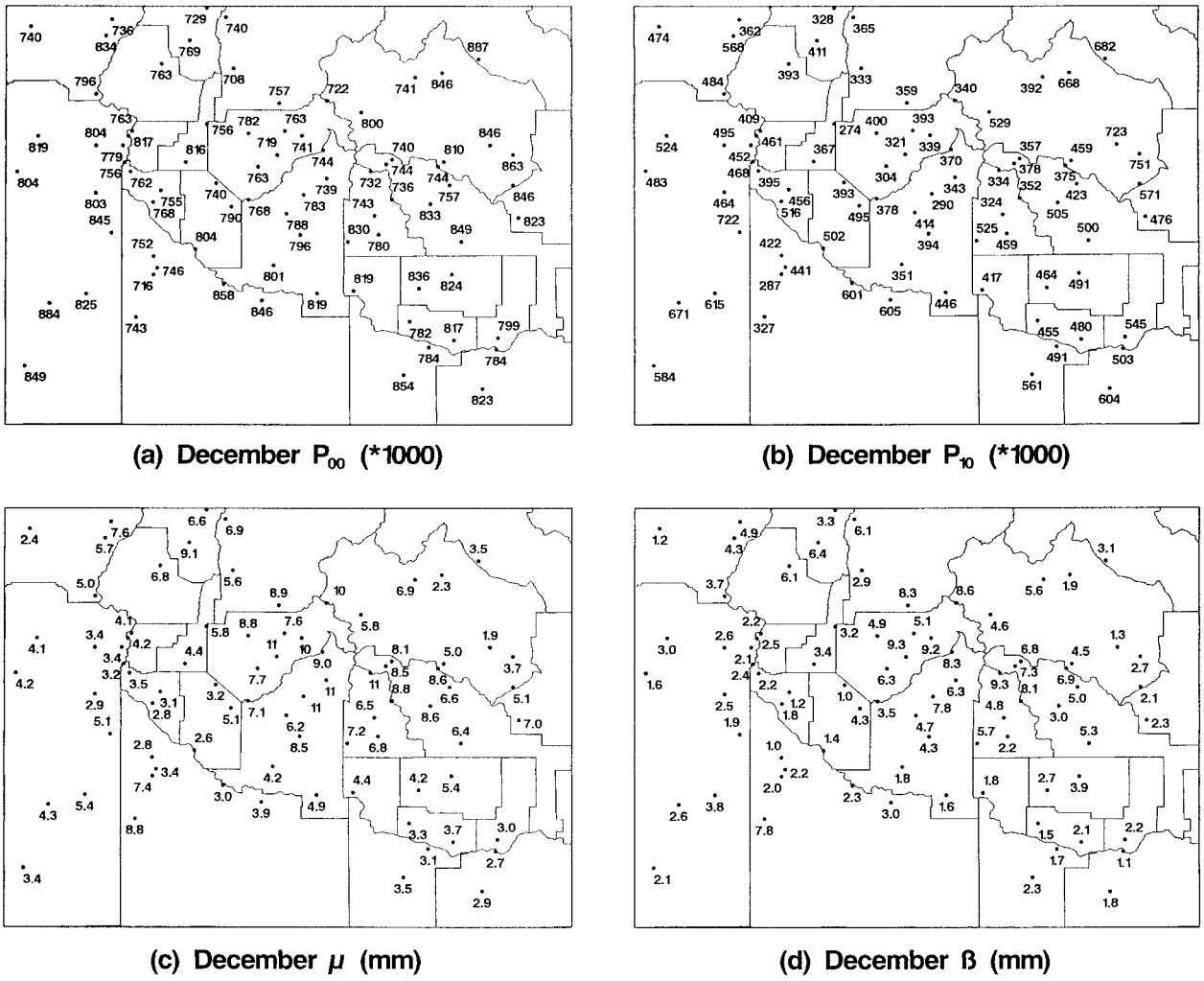

FIG. 4. Original station values of (a) p_{00}, (b) p_{10}, (c) μ and (d) β for Dec.

p_{10} decreasing with elevation in all cases (increasing persistence of wet days with elevation).

Mu, the average precipitation on a wet day, had similar local elevation relationships. At RCEW, average December μ increased from 2.8 to 7.4 mm day^{-1} with a 900-m increase in elevation, or approximately 5 mm km^{-1}. In eastern sections of the domain the μ versus elevation gradient was even more significant, especially on some leeward slopes. Beta was a much more difficult parameter to interpret because of the complex and less-than-straightforward manner in which it changed spatially. In general, β increased with local elevation (and with mean monthly and annual precipitation, as one might expect), but the change was very different from one region to another. At Reynolds Creek, December β increased just 1 mm in 900 m of elevation increase. In eastern sections of the domain, β increased at rates between 10 and 30 mm km^{-1}. Alpha had statistically insignificant change through the year at each location. Thus, a single, annual value of α was calculated and used at each location. The map of α (not shown) revealed very little spatial variability, as has been reported in earlier work (Richardson 1982), and showed no significant elevation relationship.

To illustrate the seasonal march of parameters and the influence of local elevation, the parameters p_{00}, p_{10}, μ, and β were plotted for each month of the year for the Chilly Barton Flat (lower elevation) and LostWood Divide (higher elevation) sites (Fig. 5a), only 25 km apart. Here, p_{00} shows little seasonal change, and the annual means for the two sites were nearly equal. Variability in the occurrence process for precipitation at these two sites (and at all sites in this domain) was dominated by p_{10}. From May to September, the dry season in Idaho, the difference in p_{10} at these two sites was less than 0.10. From November through March (the wet season when orographic precipitation processes are operating at their maximum), however, there was a significant elevational gradient in p_{10}, and the Lost Wood Divide site had a value nearly 0.40 lower. Thus, days following dry

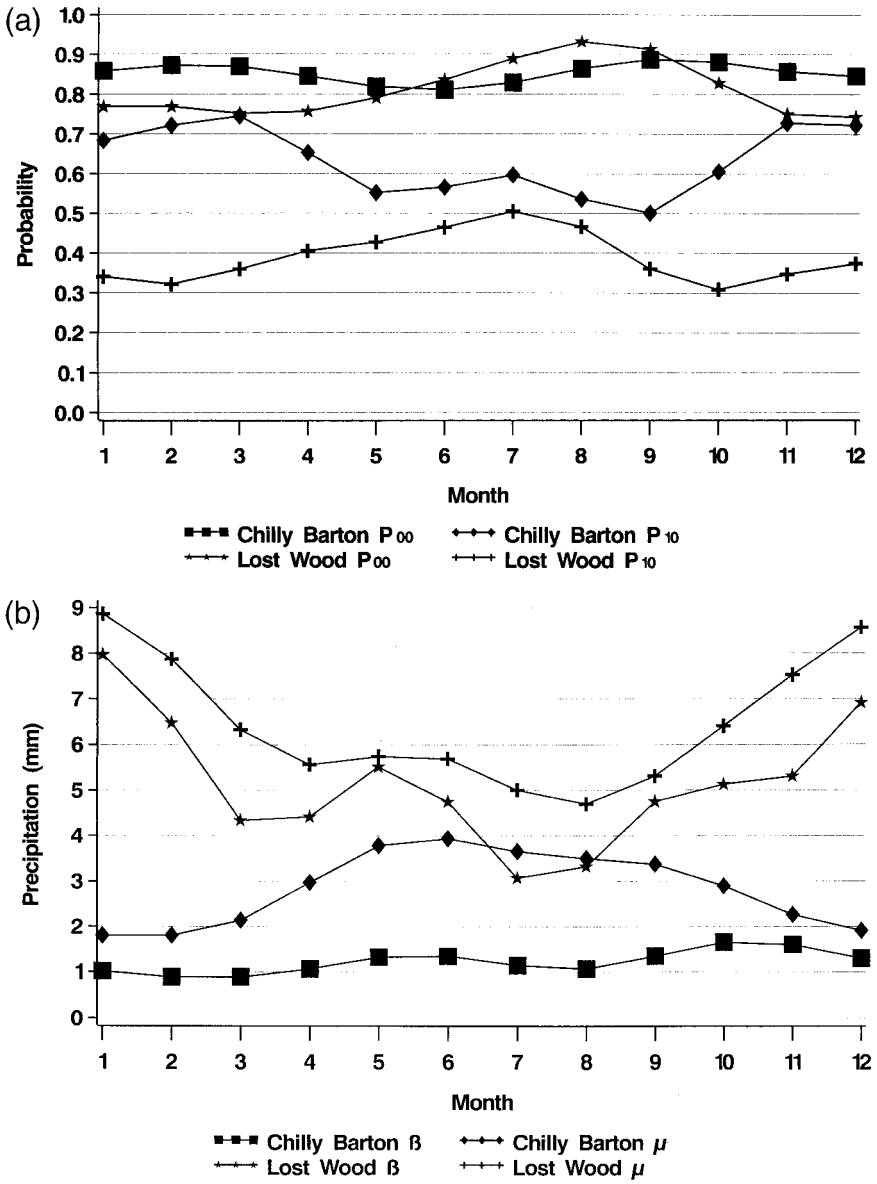

FIG. 5. Monthly time series of four precipitation parameters at lower-elevation (Chilly Barton Flat) and higher-elevation (LostWood Divide) sites in close proximity. (a) p_{00} and p_{10}; (b) μ and β.

days are about as likely to be wet or dry at any elevation; days following wet days, however, are much more likely to be wet at higher elevations. In other words, persistence of dry weather or the startup of wet weather has near-equal probability at all elevations, and persistence of wet weather is much more probable at higher elevations.

Significant differences in μ and β also were noted between the two sites (Fig. 5b). Beta had small variability at Chilly Barton, between 1 and 1.8 mm, and LostWood was always much higher and had greater month-to-month variation. The same was true for μ at LostWood, which was near 9 mm (wet day)$^{-1}$ in midwinter and decreased to less than 5 mm (wet day)$^{-1}$ in August. At Chilly Barton, μ had just the opposite characteristic, increasing from less than 2 mm (wet day)$^{-1}$ in winter to nearly 4 mm (wet day)$^{-1}$ in June. The month of June is normally one of the wettest months at all locally low–elevation sites throughout the domain, and it appears that this fact is controlled at least partially by μ and not by the occurrence process. In addition, from (1), values of δ (the mean of larger precipitation events) were derived. Although β (the mean of smaller precipitation events) increased from only 0.9 to 1.35 mm from February to June, δ increased nearly fivefold, from 1.5 to 5.16 mm. Thus, June at low elevations featured sig-

TABLE 3. Summarized PRISM interpolation statistics of monthly and annual GEM precipitation parameters. (The μ and β slopes: mm km^{-1}).

	P_{00}		P_{10}		μ (mm)		β (mm)	
Month	Slope (km)$^{-1}$	Variance	Slope (km)$^{-1}$	Variance	Slope (km)$^{-1}$	Variance	Slope (km)$^{-1}$	Variance
Jan	−0.041	0.15	−0.124	0.17	3.18	0.25	2.54	0.18
Feb	−0.043	0.18	−0.150	0.22	2.90	0.26	2.44	0.20
Mar	−0.047	0.18	−0.163	0.21	2.34	0.27	1.80	0.18
Apr	−0.049	0.21	−0.143	0.24	1.80	0.28	1.60	0.20
May	−0.049	0.30	−0.121	0.28	1.75	0.25	1.65	0.20
Jun	−0.047	0.28	−0.119	0.28	1.55	0.22	1.47	0.20
Jul	−0.039	0.26	−0.111	0.22	1.55	0.18	1.22	0.16
Aug	−0.032	0.23	−0.128	0.25	1.57	0.15	1.32	0.16
Sep	−0.028	0.20	−0.149	0.30	1.75	0.22	1.63	0.18
Oct	−0.035	0.30	−0.146	0.23	2.29	0.27	2.18	0.18
Nov	−0.043	0.17	−0.136	0.16	2.87	0.25	2.44	0.19
Dec	−0.042	0.13	−0.126	0.15	3.10	0.23	2.52	0.18

nificantly more precipitation on the wettest days than occurred on the wetter days in winter. June often has the highest atmospheric mean precipitable water values and is the most probable time for intense thunderstorm rains in this region; conditions later in the summer typically become drier and more stable.

PRISM regression slopes of precipitation occurrence parameters p_{00} and p_{10} generally were smallest in summer (Table 3). Here, p_{00} had its steepest lapse rates (change with elevation) in winter and spring, and p_{10} had two maxima corresponding to the transition months (February–April, and September and October). The greatest predictability, as denoted by r^2, was in summer. In general, the PRISM-derived regressions correctly identified the important local elevational gradients that were maximized in winter and were consistent with the domainwide predictability of p_{10} from elevation alone. The map of gridded p_{10} values in December, produced by PRISM interpolation, is shown in Fig. 6.

Mean local regression slopes from PRISM-interpolated monthly values of μ and β also were greatest (most negative) in winter and smallest in summer. In contrast to p_{00} and p_{10}, predictability was least in summer and nearly the same in all other months.

2) TEMPERATURE

Over the entire domain, some of the nine temperature parameters were related clearly to elevation, and others were related to it more poorly, as illustrated in Fig. 7. Local elevational relationships, in general, were stronger for temperature parameters than for precipitation parameters. Mean maximum temperature, separately examined for dry (Fig. 7a) and wet (Fig. 7e) days, had the most-linear elevation dependence, with domainwide r^2 values near 0.9. PRISM-interpolated average r^2 values for Tmax_d and Tmax_w were 0.62 and 0.70, respectively (Table 4). These values represent the mean r^2 of thousands of regressions (one for each of the nearly 8000 grid cells), each of which uses approximately 10–20 weighted station values.

Mean maximum temperatures were cooler on wet days than on dry days, and this difference was more pronounced with increasing elevation. Average lapse rates were approximately −4.8°C km^{-1} domainwide on dry days and approximately −6.8°C km^{-1} on wet days. Average local PRISM lapse rates were similar to these rates (Table 4). Greater lapse rates on wet days are associated with greater atmospheric mixing and stronger vertical motions.

The seasonal variation of the mean Tmax (Amp Tmax) parameter decreased with elevation domainwide ($r^2 = 0.55$; Fig. 7b) and even more so on a local basis. Amp Tmax was largest in locally low–elevation locations and across the Snake River Plain and smallest at exposed locations near or on ridges. Overall, the decrease in Amp Tmax with elevation was approximately 2°C km^{-1}, but it locally ranged from 1° to 4°C km^{-1}. The mean slope of all PRISM regressions was −2.45°C km^{-1}. This rate means that, on a local basis, the average difference in the mean maximum temperature between winter and summer decreased at a rate of nearly 2.5°C every kilometer. Thus, there was a relatively greater seasonal change in the maximum temperature of valleys versus mountaintop locations. The average r^2 of all PRISM cell regressions was 0.44.

The mean coefficient of variation (CV) of maximum temperature had very little spatial variability and was linked weakly to elevation, both domainwide ($r^2 = 0.24$; Fig. 7c) and locally. Smallest mean CV Tmax values were at the lowest and westernmost locations.

The seasonality of interdaily variability (Amp CV Tmax) was related more weakly to elevation ($r^2 = 0.10$ for the whole domain), and local elevation dependence (from PRISM regression averages) was only slightly stronger (Fig. 7d). Amp CV Tmax also had a complex spatial pattern.

Microclimatic differences were more evident in mean minimum temperatures than in mean maximum temperatures, with a domainwide elevational regression r^2 of 0.62 (Fig. 7f). In general, minimum temperature decreased with elevation domainwide, but locally the re-

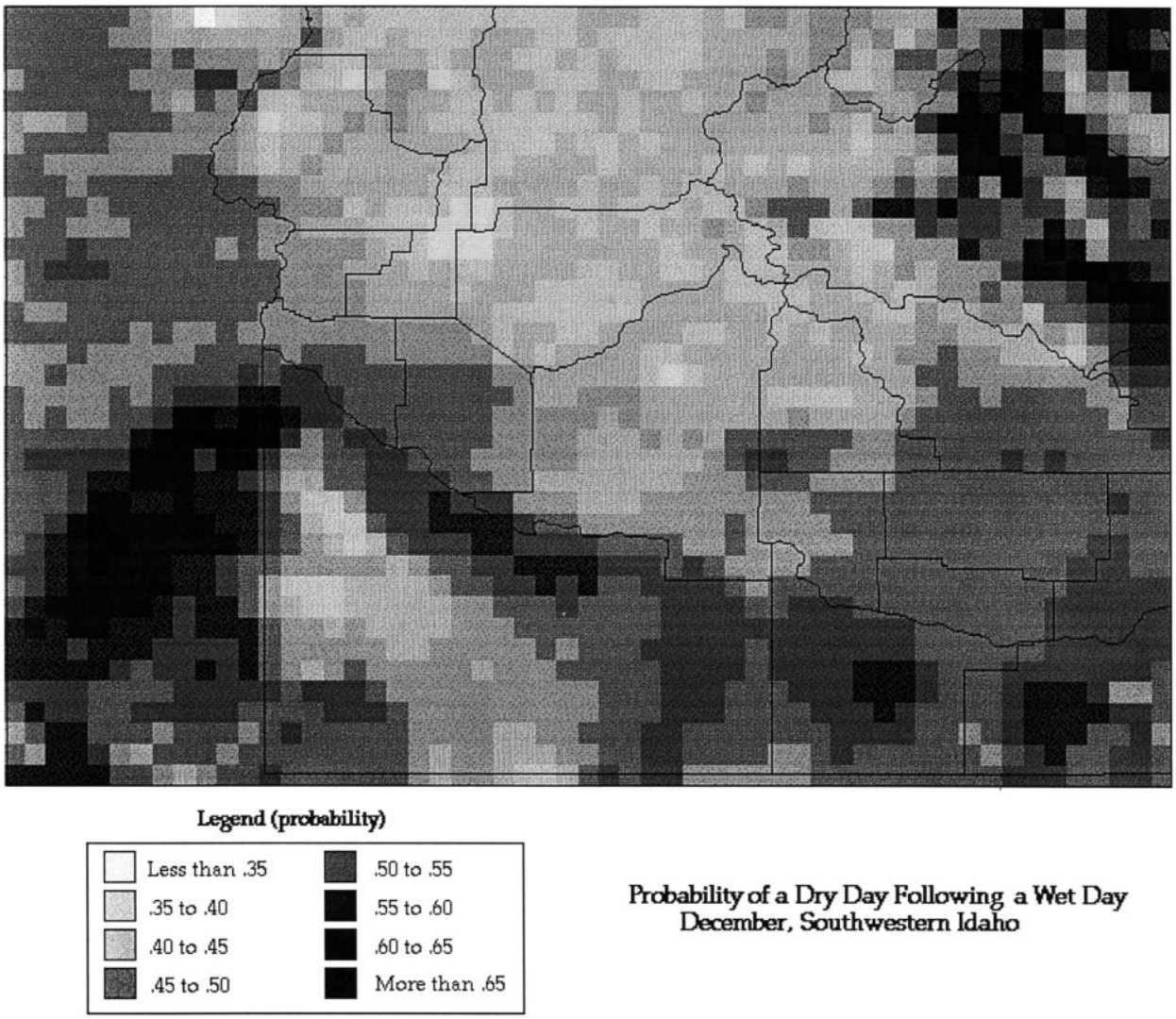

FIG. 6. PRISM-produced map of p_{10} in Dec.

lationship was anything but straightforward. For instance, at RCEW, the middle-elevation site had the warmest mean minimum, 3.4°C, due to frequent downslope warming, and the lowest-elevation site was nearly as cold as the mountaintop site (1.6°C versus 0.5°C), despite being 900 m lower in elevation. The coldest location in the domain was Stanley (−7.6°C), a dry, relatively high–elevation valley site, which was 1° to 5°C colder than all locations in the immediate vicinity, many of which were 200–800 m higher in elevation (Fig. 8).

The interpolation of Tmin parameters using PRISM presented a greater challenge than did interpolation of most Tmax parameters because of the greater microclimatic effects that typically occur at night (cold-air drainage, nocturnal winds, etc.). One of the larger-scale phenomena known to affect Tmin was a persistent temperature inversion that dominated valley locations in winter. To simulate this inversion, a feature in PRISM was developed that allows climate stations to be divided into two vertical layers, with separate regressions on each layer. Layer 1 represented the boundary layer, and layer 2 represented the free atmosphere. The thickness of the boundary layer was prescribed to reflect the height of the mean wintertime inversion height over Boise, an upper-air station near the center of this domain. Future studies will examine the prescription of different boundary layer thicknesses and its effect on the resultant temperature surfaces. The elevation of the top of the boundary layer was distributed spatially to a grid and was smoothed by using the elevation of the lowest DEM pixels in the vicinity of each pixel to develop a base layer and adding the inversion height to this elevation. As a result, large valleys and most smaller (and deeper)

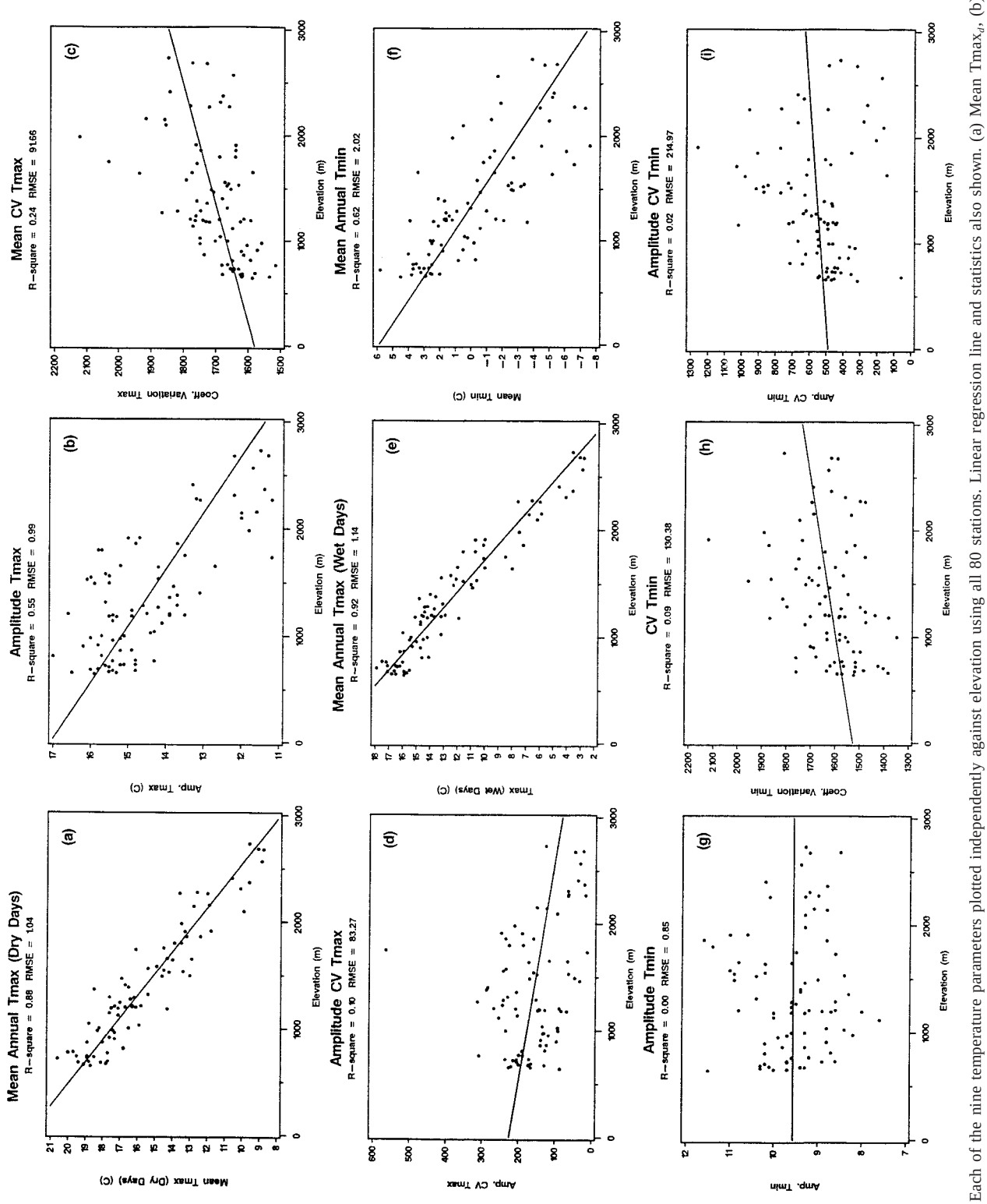

FIG. 7. Each of the nine temperature parameters plotted independently against elevation using all 80 stations. Linear regression line and statistics also shown. (a) Mean $Tmax_d$, (b) Amp Tmax, (c) mean CV Tmax, (d) Amp CV Tmax, (e) mean $Tmax_w$, (f) mean Tmin, (g) Amp Tmin, (h) mean CV Tmin, and (i) Amp CV Tmin.

TABLE 4. Summarized PRISM interpolation statistics of monthly and annual GEM temperature parameters. Slopes represent change in PRISM results versus changes in elevation.

Parameter	Vertical layer No.	Mean annual slope (km)$^{-1}$	Variance (r^2)
Mean $Tmax_d$	—	−5.33 C°	0.62
Amp Tmax	—	−2.45 C°	0.44
Mean CV Tmax	—	0.001	0.19
Amp CV Tmax	—	−0.000 95	0.16
Mean $Tmax_w$	—	−6.34 C°	0.70
Mean Tmin	1	−4.09 C°	0.29
	2	−5.14 C°	0.35
Amp Tmin	1	−0.31	0.11
	2	−0.71	0.27
Mean CV Tmin	1	0.000 15	0.11
	2	0.000 22	0.15
Amp CV Tmin	—	−0.000 12	0.05

valleys tended to fall within this layer, and local ridgetops and other elevated terrain jutted into the free atmosphere (Fig. 9).

To accommodate the spatially and temporally varying strength of the inversion, PRISM was designed to allow varying amounts of ''cross talk'' (sharing of data points) between the vertical layer regressions, depending on the similarity of the regression functions. Under strong inversion conditions in winter, the regression functions would be very different, and cross talk between the two layers would be minimized. During summer and in well-mixed locations, the regression functions would show similar characteristics, and stations would be shared more freely across the layer 1–layer 2 boundary. PRISM examined these functions and made a determination of the appropriate level of cross talk required.

The mean elevational regression slope (Table 4) of Tmin in the lower layer was −4.09°C km^{-1} and, as expected, was more negative in layer 2 (−5.14°C km^{-1}). PRISM r^2 values for layers 1 and 2 were 0.29 and 0.35, respectively. The inclusion of a two-layered approach to mean annual Tmin interpolation improved the results over approaches without consideration of a mean inversion top, but other factors would have to be included to replicate more accurately Tmin in all locations. The final PRISM-produced map of annual mean Tmin captured nearly all of the significant spatial variabilities at the chosen modeling scale (Figure 10), however. The numerous cold pockets in the mountains were depicted well, as were the highest mountains and all valleys, even in regions where there were relatively little observational data.

The mean value of the amplitude of the first harmonic of Tmin had a significantly smaller lapse rate for both PRISM layers 1 (−0.31°C km^{-1}) and 2 (−0.71°C km^{-1}) in comparison with the average PRISM lapse rate of the amplitude of Tmax (−2.45°C km^{-1}). Locally, there was a slight elevational gradient in the seasonal change (annual amplitude) of Tmin, with greatest seasonal changes at lower elevations. Actual station values had negligible elevation dependence domainwide (Fig. 7g), again emphasizing the need for a locally based elevation regression approach such as is used in PRISM. In general, this parameter was lowest in the western section of the domain and highest in the eastern section. Greatest values were found at locations in the eastern plateau and in relatively deep valleys throughout. These locations are subject to relatively cold winter nights in comparison with locations further west at similar elevation. This

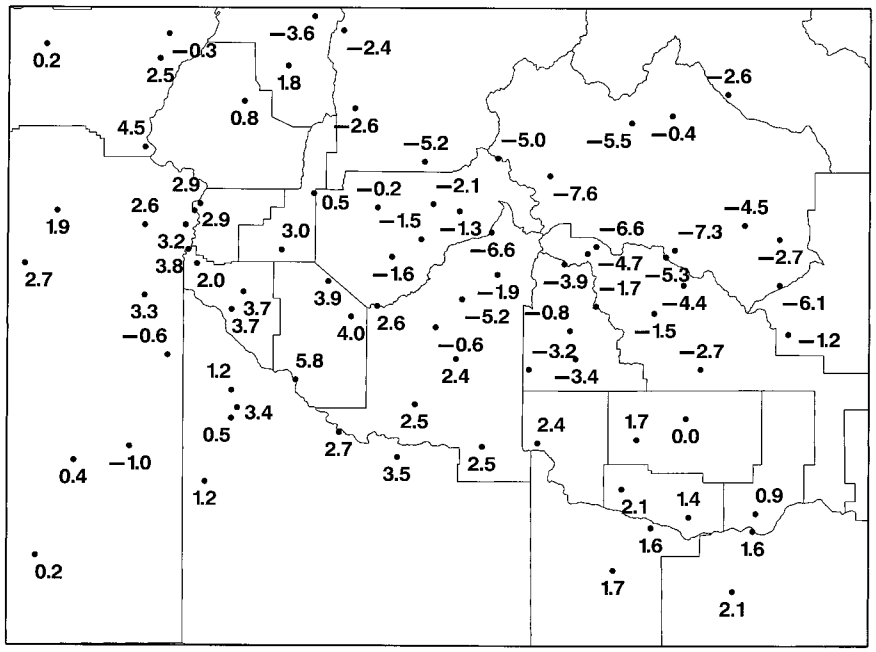

FIG. 8. Observed mean annual Tmin values (°C) at all 80 stations in the domain.

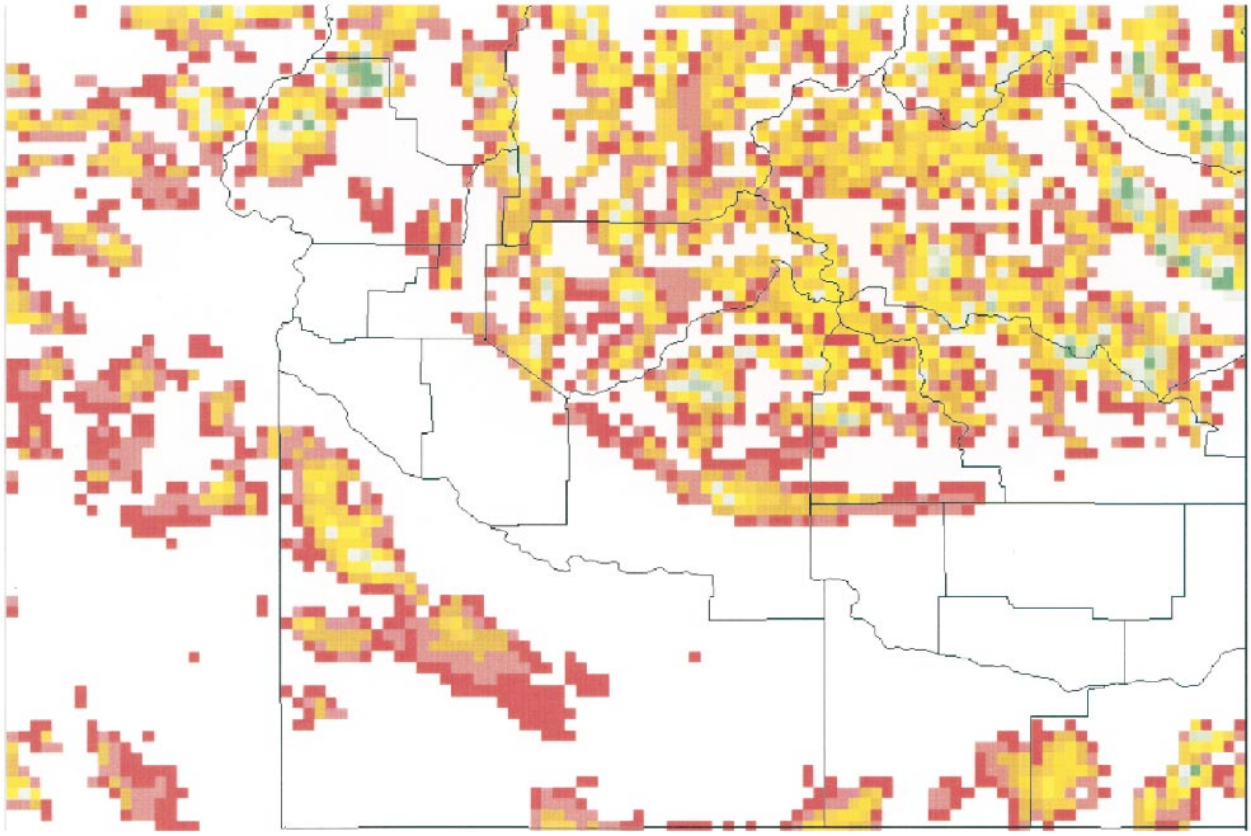

FIG. 9. Cell heights above or below the smoothed elevation surface–plus–250-m height, used in the two-layer atmosphere method for mapping minimum temperature parameters with PRISM over the study domain. No color (white) indicates cells at or below this surface. Red is approximately 100 m above the mean inversion height; yellow is approximately 250 m; and green is approximately 400 m.

difference may represent increasing continentality and decreasing influence of Pacific weather systems with eastward movement across the domain.

The mean annual coefficient of variation of Tmin (mean CV Tmin) was uniform spatially, with no appreciable elevational dependence (domainwide $r^2 = 0.09$; mean of PRISM regressions $r^2 = 0.13$). Slopes of domainwide and PRISM regressions also were negligible (Fig. 7h; Table 4). The largest values were found at moderately high–elevation, dry valleys such as the Stanley Basin, with maximum potential radiational cooling and cold-air drainage. The seasonal variation of this parameter, represented by Amp CV Tmin, was tied closely to mean CV, with the largest absolute values also at Stanley and other moderately high valleys and plateau locations. In general, this parameter increased in variability with increasing elevation. Domainwide, elevational dependence was near zero (Fig. 7i); on a local basis, however, there was a slightly greater relationship (Table 4). In short, variability about the mean daily minimum temperature exhibited a relatively greater seasonal change, that is, between summer (less at all sites) and winter (greater at all sites), with increasing elevation and westward position in this domain. This result is opposite to the elevational gradient of the seasonal change of mean Tmin.

5. PRISM validation statistics

Overall performance of PRISM was evaluated using several criteria, including bias and mean absolute error (MAE) statistics, as described by Daly et al. (1994). Bias was calculated as

$$\text{bias} = \frac{1}{n}\sum_{i=1}^{n}(P_i - O_i), \tag{2}$$

where P_i and O_i are the generated (predicted) and observed precipitation for the ith station, respectively. MAE was defined as

$$\text{MAE} = \frac{1}{n}\sum_{i=1}^{n}|P_i - O_i|. \tag{3}$$

Bias and (MAE) jackknife cross-validation statistics [see Daly et al. (1994) for explanation] for all 58 interpolated parameters were computed and given as both actual values. and as percentages (Table 5). Percentages are calculated by expressing each error as a percentage

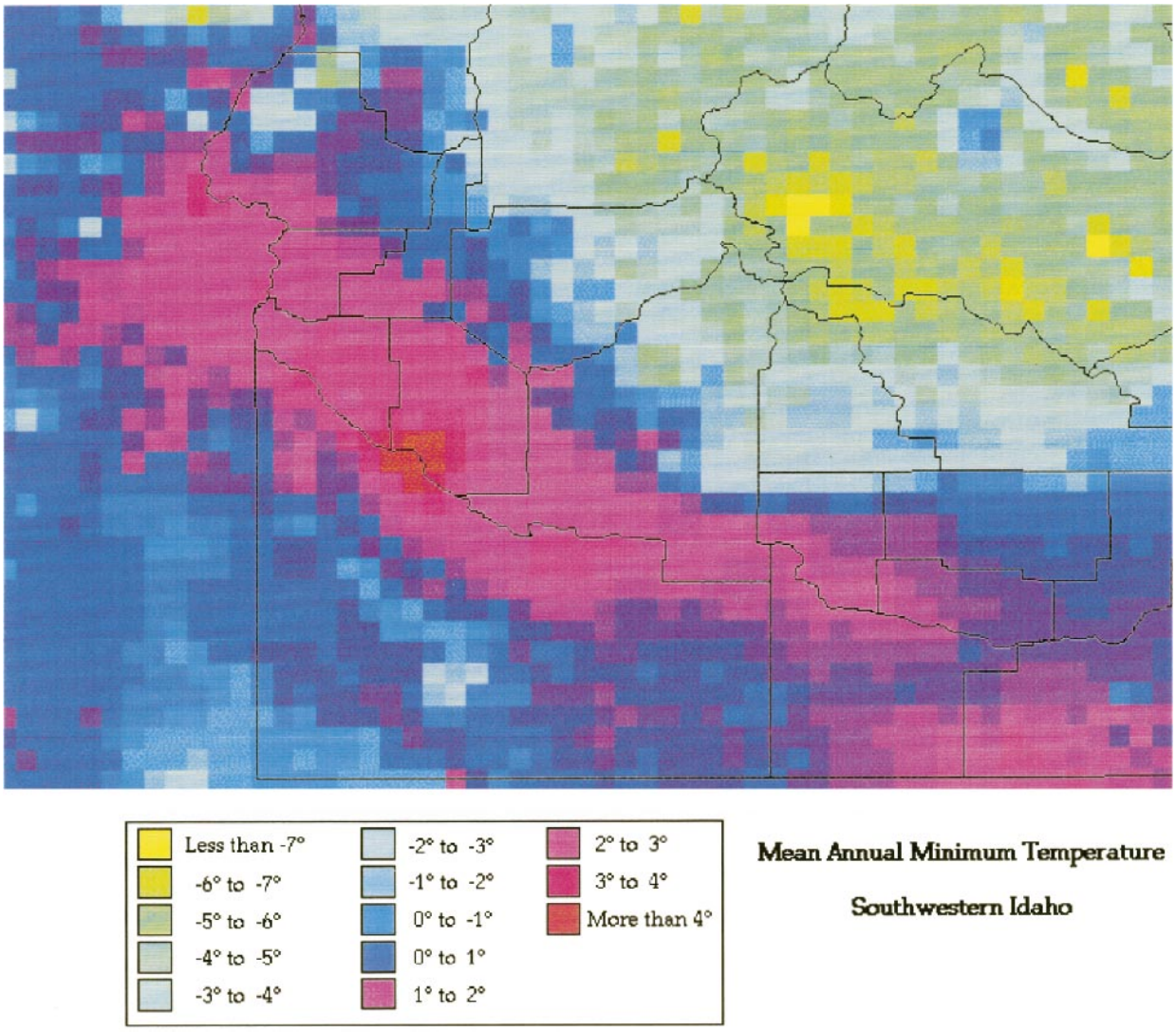

FIG. 10. Annual mean minimum temperature (°C) grid map produced by PRISM over the study domain.

of the observation and then averaging the percentages. Percentage statistics are not given for temperature parameters, because they are somewhat meaningless because of the choice of temperature scale (Celsius), for which negative, positive, and zero values all are possible.

These statistics confirmed many of the hypotheses discussed above. Best overall model performance based on these four criteria was for p_{00}, mean Tmax_d and Tmax_w, mean Tmin, and Amp Tmax. The largest error statistics were noted for those parameters that were discussed above as being difficult to interpolate, often with no clear elevational or geographic dependencies. These parameters included β, Amp CV Tmax, and Amp CV Tmin. Beta, in particular, is a parameter that showed highly local dependencies, in addition to regional and elevational gradients (Fig. 4d), and reasons for its sometimes erratic spatial behavior were not readily apparent.

PRISM-interpolated p_{00} and p_{10} bias values were extremely small, and percent biases were mostly less than 1%. Percentage MAEs of the conditional probabilities also were low, except for a value of a little more than 10% for p_{10} in the winter months.

6. Conclusions and applications

In an effort to generate climate time series at locations with no recorded climate history and/or in regions with spatially nonhomogeneous climate, a study was undertaken to examine the spatial variability of the parameters of a stochastic weather generator model and to determine the feasibility of using the PRISM modeling system to distribute these parameters to a high-resolution (2.5 min. or approximately 3 km $\times$ 5 km at this latitude) grid. First, methods were devised to develop a set of GEM weather generator parameters for climate stations

TABLE 5. PRISM jackknife cross-validation statistics for all 58 parameters. Percentage values are averages of values at all locations. Maximum and minimum values of each parameter are shown in bold.

Parameter/month	Bias	MAE	Percent bias	Percent MAE
α		0.032	2.98	13.8
β	0.0017			
1	−0.0031	**0.048**	19.70	45.23
2	−0.0030	0.044	**27.30**	**54.03**
3	−0.0011	0.039	23.32	50.71
4	−0.000 67	0.034	20.58	46.21
5	−0.0039	0.034	13.86	42.85
6	**−0.0041**	0.031	**12.50**	37.92
7	0.000 29	0.030	15.04	37.56
8	**0.0014**	**0.028**	13.00	**34.09**
9	−0.000 90	0.032	14.89	39.51
10	**−0.0041**	0.040	17.57	45.84
11	−0.0035	0.039	14.89	39.66
12	−0.0017	0.042	14.62	37.27
μ				
1	**−0.0038**	**0.046**	5.74	**23.86**
2	−0.0031	0.035	4.69	20.15
3	−0.0019	0.029	3.85	18.11
4	0.000 44	0.024	2.42	13.72
5	0.0013	**0.022**	**2.05**	**12.02**
6	0.000 89	0.023	2.22	13.41
7	0.0015	0.027	3.22	16.00
8	**0.0034**	0.030	4.38	17.25
9	0.000 74	0.023	2.48	12.94
10	−0.000 33	0.028	3.04	14.78
11	−0.0029	0.036	4.28	19.87
12	−0.0033	0.044	**5.83**	23.17
p_{00}				
1	−0.0036	0.021	**−0.34**	2.63
2	−0.0032	0.020	−0.30	2.49
3	−0.0033	0.020	−0.32	2.40
4	−0.0024	0.016	−0.23	2.01
5	−0.000 15	0.014	0.03	1.71
6	**−0.000 02**	0.015	**0.03**	1.69
7	−0.000 42	0.011	−0.03	1.23
8	−0.0014	**0.010**	−0.13	**1.12**
9	−0.000 82	0.011	−0.07	1.14
10	−0.000 80	0.012	−0.07	1.33
11	−0.0028	0.020	−0.27	2.54
12	**−0.0037**	**0.025**	−0.32	**3.20**
p_{10}				
1	−0.0039	0.050	**1.42**	11.82
2	−0.0050	0.054	1.32	11.99
3	−0.0076	0.060	0.84	12.51
4	−0.0047	0.050	0.71	9.92
5	−0.000 80	**0.036**	0.75	7.31
6	**−0.000 24**	**0.036**	0.58	6.65
7	−0.0039	0.040	−0.03	6.69
8	−0.0048	0.040	**−0.16**	**6.58**
9	−0.0063	0.046	−0.10	8.39
10	−0.0070	0.058	0.80	11.96
11	**−0.010**	**0.064**	0.73	**13.58**
12	−0.0048	0.055	1.36	12.49
Mean $Tmax_d$	−0.13	0.86	—	—
Amp Tmax	0.002	0.60	—	—
Mean CV Tmax	0.000 008 2	0.000 62	—	—
Amp CV Tmax	−0.000 006 5	−0.000 47	—	—
Mean $Tmax_w$	−0.18	1.00	—	—
Mean Tmin	−0.041	1.47	—	—
Amp Tmin	0.015	0.49	—	—
Mean CV Tmin	−0.000 056	0.000 98	—	—
Amp CV Tmin	−0.000 052	−0.0015	—	—

with dissimilar measurement standards. Then, point parameter values were used by PRISM to develop gridded fields of each of the 58 parameters necessary to generate daily precipitation and temperature time series using GEM at any grid cell.

Most precipitation and temperature parameters of the GEM weather generator model were found to be topographically dependent and were interpolated successfully to grid points using the PRISM model. In most cases, statistical bias and mean absolute errors were small, especially relative to the generated values in a time series. The largest values in terms of percentage of the observations were for the β parameter, with MAE percentages between 34% and 54%. New methodologies were developed to map minimum temperature parameters, which can have significant local effects because of persistent cold-air drainage problems and consequent inversions. In general, this study has proven the capabilities of the PRISM modeling system for distributing these types of parameters to grid points and the potential for using this system to generate daily time series of any length, even at very remote and/or high-elevation locations. The potential applicability of this methodology to the hydrologic and natural resource sciences is considerable.

A prototype system has been developed whereby users select any location in the test region, extract all necessary GEM parameters from that location, and then generate a daily time series for a specified length of time using GEM. PRISM layers are linked geospatially. Several screens of information prompt users for site selection, elements to generate, and period length. A map of the region is shown, and users then may use the cursor to select a location or enter the latitude and longitude manually. After several other screens that request additional information, a daily time series is generated, that may be viewed or saved to a file.

This system is being reviewed by natural resource management agencies for implementation at field offices and for providing the necessary climate inputs for many natural resource models of various applications, including wind erosion, soil moisture and temperature estimation, and crop and natural vegetation growth.

Future efforts will focus on refining the methodology, testing it in other regions, and expanding the number of climate elements distributed using PRISM and generated by GEM, including dewpoint, solar radiation, and, possibly, wind speed and direction.

Acknowledgments. The authors are deeply appreciative of the significant efforts of Yunyun Lu and Ward Ballard in gathering the data necessary for this study, deriving the GEM parameters, assisting with data analysis, and preparing the figures and tables in this manuscript.

APPENDIX

SNOTEL Precipitation Parameter Estimation

GEM parameter derivation using data from the USDA Natural Resources Conservation Service's SNOTEL network was not straightforward because of the use of a 2.5-mm minimum threshold for precipitation measurement at these sites, rather than the 0.25 mm used by all other networks. Although monthly and annual totals were not affected, the number of wet days per year (and also for other time increments) and the average amount of precipitation per wet day (directly affecting the computed values of p_{00}, p_{10}, μ, α, and β used in GEM) were different. AGUA assumed a measurement standard for precipitation of 0.25 mm (Todorovic and Woolhiser 1975; Hanson et al. 1994). Therefore, a procedure was developed to estimate these parameters at SNOTEL sites through relationships with total precipitation.

Second-order polynomial equations of p_{00}, p_{10}, and μ versus total period precipitation were first derived using all NOAA and ARS stations (combined over the entire domain) for each 14-day period of the calendar year (26 periods). An example of p_{10} versus mean December precipitation is shown in Fig. 1 (in this case, showing all 80 stations, including SNOTEL sites). Next, mean precipitation for each of these 26 periods was calculated at each SNOTEL station using the number of years of available data (generally 5–10). Using these mean period precipitation values and the equations, values for p_{00}, p_{10}, and μ were estimated for each period for each SNOTEL station. Mean period values for α and β were derived from the raw SNOTEL daily data using a separate subroutine in AGUA. All of these initial period values then were used to derive an annual Fourier series with annual mean and first three harmonics of each parameter (Woolhiser and Pegram 1979). Thus, initial, or first-guess values that describe the seasonal variation of p_{00}, p_{10}, μ, α, and β were derived. Then, using the following formula, an initial estimate of mean annual precipitation (MAP) for each SNOTEL site was made:

$$E(\text{MAP}) = \sum_{n=1}^{365} \{P[x(n) = 1]\} \times \{\alpha(n)\beta(n) + [1 - \alpha(n)]\delta(n)\}, \quad \text{(A1)}$$

where E(MAP) is expected mean annual precipitation, $P[x(n)] = 1$ is the unconditional probability that the previous day n was wet and is approximately equal to

$$\frac{1 - p_{00}(n)}{1 + p_{10}(n) - p_{00}(n)}, \quad \text{(A2)}$$

x is a random variable that represents the occurrence or nonoccurrence of precipitation on day n, and

$$\delta(n) = \frac{\mu(n) - \alpha(n)\beta(n)}{1 - \alpha(n)}. \quad \text{(A3)}$$

This E(MAP) value was compared with the known MAP for the station (based on the raw SNOTEL data), and, if the difference was greater than 25 mm, a Newton–Raphson iterative procedure was invoked until the difference became smaller than 25 mm. Details of this iteration are given on p. 11 of Hanson et al. (1994) but, in short, only mean annual values of p_{10} and α were used for adjustment.

Once initial and adjusted parameters were obtained, a 30-yr daily precipitation time series was generated using GEM. Annual and period mean parameter and total precipitation values were derived from this generated output using the standard GEM parameterization program (using the generated values as if they were actual observations). The generated mean precipitation values for each of the 26 discrete time periods were compared with the original values from the second step, described above. For all periods in which the difference was greater than a prescribed threshold (in this case, 10 mm), values of p_{00}, p_{10}, and μ were adjusted using an adjusted mean period precipitation amount given by

$$\text{ADJPP} = \text{ORIGPP} + 0.5(\text{ERRPP}), \qquad \text{(A4)}$$

where ADJPP is the period precipitation used in the new iteration, ORIGPP is the original mean period precipitation amount (from the second step, above), and ERRPP is the difference between ORIGPP and the mean period precipitation derived from the 30-yr GEM simulation. With these adjusted parameter values, the entire iterative procedure was conducted again, starting with the second step, described above. This process was repeated until final parameter values delivered GEM-generated mean annual and period precipitation meeting the criteria set forth above.

REFERENCES

Daly, C., R. P. Neilson, and D. L. Phillips, 1994: A statistical–topographic model for mapping climatological precipitation over mountainous terrain. *J. Appl. Meteor.,* **33,** 140–158.

——, G. H. Taylor, and W. Gibson, 1997: The PRISM approach to mapping precipitation and temperature. Preprints, *10th Conf. on Applied Climatology,* Reno, NV, Amer. Meteor. Soc., 10–12.

Foufoula-Georgiou, E., and D. P. Lettenmaier, 1987: A Markov renewal model for rainfall occurrences. *Water Resour. Res.,* **23,** 875–884.

Hanson, C. L., and G. L. Johnson, 1998: GEM (Generation of Weather Elements for Multiple Applications): Its application in areas of complex terrain. *Hydrology, Water Resources and Ecology in Headwaters—Proc. HeadWater '98 Conf.,* Meran, Italy, International Association of Hydrological Sciences, 27–32.

——, K. A. Cumming, D. A. Woolhiser, and C. W. Richardson, 1994: Microcomputer program for daily weather simulation. USDA Agricultural Research Service Publication ARS-114, 38 pp. [Available from U.S. Dept. of Agriculture, Agricultural Research Service, 800 Park Blvd., Plaza IV, Suite 105, Boise, ID 83712-7716.]

Hayhoe, H. N., 1998: Relationship between weather variables in observed and WXGEN generated data series. *Agric. For. Meteor.,* **90,** 203–214.

Johnson, G. L., C. L. Hanson, S. P. Hardegree, and E. B. Ballard, 1996: Stochastic weather simulation: Overview and analysis of two commonly used models. *J. Appl. Meteor.,* **35,** 1878–1896.

Katz, R. W., 1996: Use of conditional stochastic models to generate climate change scenarios. *Climatic Change,* **32,** 237–255.

Kittel, T. G. F., and Coauthors, 1997: A gridded historical (1895–1993) bioclimate dataset for the conterminous United States. Preprints, *10th Conf. on Applied Climatology,* Reno, NV, Amer. Meteor. Soc., 219–222.

Matalas, N. C., 1967: Mathematical assessment of synthetic hydrology. *Water Resour. Res.,* **3,** 937–945.

Mearns, L. O., C. Rosenzweig, and R. Goldberg, 1996: The effect of changes in daily and interannual climatic variability on CERES-Wheat: A sensitivity study. *Climatic Change,* **32,** 257–292.

Nicks, A. D., and G. A. Gander, 1994: CLIGEN: A weather generator for climate inputs to water resource and other models. *Proc. Fifth Int. Conf. on Computers in Agriculture,* Orlando, FL, American Society of Agricultural Engineers, 903–909.

Parlange, M. B., and R. W. Katz, 2000: An extended version of the Richardson model for simulating daily weather variables. *J. Appl. Meteor.,* **39,** 610–622.

Parzybok, T., W. P. Gibson, C. Daly, and G. H. Taylor, 1997: Quality assurance of climatological data for the VEMAP Project. Preprints, *10th Conf. on Applied Climatology,* Reno, NV, Amer. Meteor. Soc., 215–216.

Richardson, C. W., 1981: Stochastic simulation of daily precipitation, temperature, and solar radiation. *Water Resour. Res.,* **17,** 182–190.

——, 1982: Dependence structure of daily precipitation, temperature and solar radiation. *Trans. ASAE,* **25,** 735–739.

——, and D. A. Wright, 1984: WGEN: A model for generating daily weather variables. USDA Agricultural Research Service Publication ARS-8, 83 pp. [Available from U.S. Dept. of Agriculture, Agricultural Research Service, 808 E. Blackland Rd., Temple, TX 76502.]

Smith, R. E., and H. A. Schreiber, 1974: Point processes of seasonal thunderstorm rainfall. Part 2: Rainfall depth probabilities. *Water Resour. Res.,* **10,** 418–423.

Taylor, G. H., C. Daly, W. P. Gibson, and J. Sibul-Weisberg, 1997: Digital and map products produced using PRISM. Preprints, *10th Conf. on Applied Climatology,* Reno, NV, Amer. Meteor. Soc., 217–218.

Todorovic, P., and D. A. Woolhiser, 1975: A stochastic model of n-day precipitation. *J. Appl. Meteor.,* **14,** 17–24.

Wilks, D. S., 1998: Multisite generalization of a daily stochastic precipitation generation model. *J. Hydrol.,* **210,** 178–191.

Woolhiser, D. A., and G. G. S. Pegram, 1979: Maximum likelihood estimation of Fourier coefficients to describe seasonal variations of parameters in stochastic daily precipitation models. *J. Appl. Meteor.,* **18,** 34–42.

——, and J. Roldan, 1982a: Stochastic daily precipitation models, Part 1. A comparison of occurrence processes. *Water Resour. Res.,* **18,** 1451–1459.

——, and ——, 1982b: Stochastic daily precipitation models, Part 2. A comparison of distributions of amounts. *Water Resour. Res.,* **18,** 1461–1468.

——, and ——, 1986: Seasonal and regional variability of parameters for stochastic daily precipitation models: South Dakota, U.S.A. *Water Resour. Res.,* **22,** 965–978.

——, C. L. Hanson, and C. W. Richardson, 1988. Microcomputer program for daily weather simulation. USDA Agricultural Research Service Publication ARS-75, 49 pp. [Available from U.S. Dept. of Agriculture, Agricultural Research Service, 800 Park Blvd., Plaza IV, Suite 105, Boise, ID 83712-7716.]